Caspian Journal of Environmental Sciences
Online ISSN: 1735-3866
Print ISSN: 1735-3033

Evaluation the anticancer and biological activity by new amide compound of trimethoprim with some of its complexes

Alaa Abdullah Majeed*, Asmaa Mohammed Noori Khaleel

Department of Chemistry, College of Science, University of Baghdad, Baghdad, Iraq

** Corresponding author's E-mail: alaaabdulla132@gmail.com*

ABSTRACT

By reacting trimethoprim and hippuric acid at a molecular weight of 1, the amide ligand molecule was produced. By reacting ligands with $CoCl_2.2H_2O$, $NiCl_2.6H_2O$, and K_2PtCl_6 in a 2:1 [L:M] mole ratio, cobalt (II), nickel (II), and platinum (IV) complexes were produced. All of the produced compounds were studied by taking readings of their FT-IR, UV-Vis, TG/DTA, 1H-NMR, CHN, melting point, molar conductivity, magnetic susceptibility, and chloride. All the synthesized compounds had anticancer, antibacterial, and antifungal activities against *Staphylococcus aureus*, *Pseudomonas aeruginosa*, and *Candida*, respectively.

Keywords: Drug, Trimethoprim, Amide structure, Hippuric acid, Anticancer.
Article type: Research Article.

INTRODUCTION

Trimethoprim and other heterocyclic compounds play an important role in the pharmaceutical and medical fields. The vast majority of new medications, including imipramine (Eicher & Hauptmann 2003) and indapamide (UK Food Standards Agency 2008), have an amide structure and are therefore classified as heterocyclic compounds. Amide is obtained as a starting material for the synthesis of novel complexes involving trimethoprim amides and maleimide derivatives (Merrill & Henderson 1999). When it comes to treating inflammatory diseases like arthritis, heterocyclic compounds are the first line of defence (Aljeboree *et al.* 2023). They are important pharmacoactive agents in medicinal chemistry (Cooper *et al.* 2007). It is common knowledge that trimethoprim is an excellent antibacterial agent (Skerritt & Johnston 1993). Antibiotics are also prescribed to treat bacterial infections of the urinary system, upper respiratory tract, lungs, and throat, as well as conditions including chronic bronchitis and pneumonia (Mayo 2002). Hippuric acid has many well-documented pharmacological effects, including those of an antibacterial, antifungal, antimycobacterial, antiviral, antileishmanial, anticancer, anti-inflammatory, analgesic, antihypertensive, anticonvulsant, anti-oxidant, anti-diabetic, ulcerogenic, and many other drugs (Mutschler 1995). Urine contains hippuric acid, an acyl glycine forms from the conjugation of benzoic acid and glycine, which is a common metabolite of dietary aromatic chemicals. Potential antimicrobial effects of elevated hippuric acid in urine Hippurate salts (calcium and ammonium) of hippuric acid are utilized medicinally (Guyton & Hall 1975; Goldstein 2002). To boost its biological and medicinal efficacy, we have synthesized a novel amide ligand by combining trimethoprim and hippuric acid. To further improve its biological and medicinal utility, we are also synthesizing metal complexes of this amide ligand with Co (II), Ni (II), and Pt (IV) metal ions. Physicochemical and spectroscopic characterization of all produced molecules to validate the proposed structure (Capasso C & Supuran 2014; Amdare *et al.* 2017; Qassem & Jassim 2021) The chemical synthesized was evaluated for its potential biological and therapeutic effects.

MATERIALS AND METHODS

Iodine was used in conjunction with the thin layer chromatography (TLC) method with the solvents chloroform, acetic acid, and toluene (2:3:1). A Gallenkamp melting point device was used to measure the melting points of all

Caspian Journal of Environmental Sciences, Vol. 22 No. 1 pp. 9-22 Received: July 17, 2023 Revised: Sep. 09, 2023 Accepted: Nov. 27, 2023
DOI: 10.22124/cjes.2023.7323

Publisher: University of Guilan,

the compounds. FTIR (Fourier Transform Infrared) measurements were taken with a SHIMADZU 8400s Spectrophotometer between 400 and 4000 cm^{-1} (KBr) for the ligands, and between 250 and 4000 cm^{-1} (KBr) for the complexes (CsI). Using DMSO as a solvent, UV-visible spectra were taken using a Shimadzu 1800 UV spectrophotometer in the wavelength range of 190–1100 nm. The ^{1}H-NMR spectra in DMSO were obtained using a Bruker 600 MHz NMR Spectrometer. Thermographic and dimensional thermal analyses (TG and DTA) were documented by the Mettler TA 4000 System. Using a Nova 350 Spectrophotometer, metal concentrations were determined by flame atomic absorption spectroscopy. Auto-Magnetic Susceptibility Balance Model Sherwood Scientific was used to record magnetic susceptibility and molar conductivity at room temperature. The complexes' chloride levels were determined using the Mohr technique. The Elemental Analyzer EuroEA 3000/Italy was used to record the results of microscopic elemental analyses (CHN). Agar diffusion was used to test for antimicrobial activity. Testing for anticancer properties in cell lines was conducted at Iraq's Cell Bank Unit for Biotechnology.

Synthesis N-(2-((2-amino-4-((3,4,5-trimethoxycyclohexa-1,3-dien-1-yl)methyl)pyrimidin-5-yl) (methyl) amino)-2-oxoethyl)benzamide (L)

A solution of trimethoprim (0.1 g, 0.344 mmol) in 6 mL methanol was added to hippuric acid solution (0.0617 g, 0.344 mmol) in 2 mL methanol, and the mixture was heated for 5 min while being stirred to ensure complete solubility. The mixture was then refluxed for 8 h. After examining the solution by thin-layer chromatography, we evaporated a part of the solvent by heating. The substance was collected by crushing in an ice bath, then washed in acetone and dried in an oven to produce a white powder (Fig. 1; Chiu *et al.* 2021).

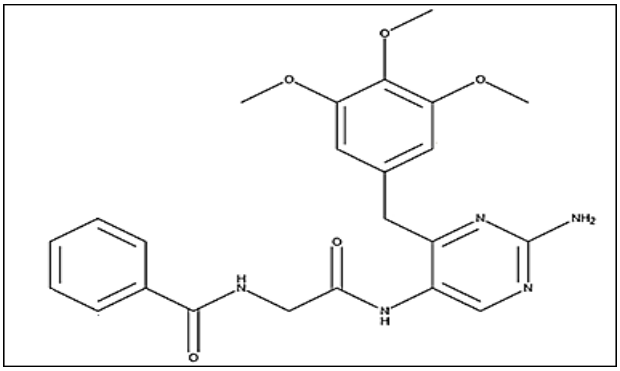

Fig. 1. Ligand structure.

2.2 Synthesis Ni (II), Co (II) and Pt (IV) complexes (C_1, C_2 and C_3)

The mixture of ligand (0.1 g, 0.221 mmol) in 4-mL water and metal salts (Table 1) in 2-mL water was prepared as (2:1 L:M), and then the mixture was heated under reflux for 5 h with stirring. We evaporated a part of the solvent by heating. The substance was collected by crushing it in an ice bath of solvent heating, then washed in ice water and dried in an oven.

Table 1. The optimization conditions for synthesis of complexes.

No	Ligand [wt(g), mmol] in 2 mL H_2O	Metal salts [wt(g), mmol] in 4 mL H_2O	Color of preceptate	Color of solution
C_1 Co(II)	L (0.1g, 0.221 mmol)	[$CoCl_2.6H_2O$](0.0216 g, 0.09 mmole)	pale blue	reddish pink
C_2 Ni(II)	L (0.1g, 0.221 mmol)	[$NiCl_2.6H_2O$](0.0143 g, 0.11 mmole)	Light green	green
C_3 Pt(IV)	L (0.1g, 0.221 mmol)	[K_2PtCl_6] (0.0538 g, 0.11mmole)	brown	yellow

Anticancer

Each well in a 96-well microtiter plate contained a total of 200 mL of full culture media for the tumour cells. Parafilm was used to keep the microplate sterile, and it was gently shaken. After incubating the plates for 24 h at 37 ℃ with 5% carbon dioxide (72 h), two-fold dilutions of the target chemicals (50, 100, 200 and 400 mg mL^{-1}) were added to the wells, and after incubation was complete, the medium was discarded. Each concentration

and the controls were tested in triplicate (cells treated with serum-free medium). After predetermined exposure times, plates were incubated at 37 ℃with 5% carbon dioxide for 72 h.

Antimicrobial activities

All synthesized compounds were evaluated according to the antibacterial action against *Pseudomonas aeruginosa* and *Staphylococcus aureus*, as well as the *Candida* fungus, when tested at 10^{-2} M in DMSO solutions using the agar diffusion method. Inhibition radii were used to determine the efficacy against bacteria and fungi.

RESULT AND DISCUSSION

Physical properties and elemental microanalysis

The data of metal content (atomic absorption), CHN, the physical properties and the name of the ligand and its metal complexes are shown in Table 2. The molecular formulae of studied compounds were suggested depending on CHN, atomic absorption analysis, chloride content, spectral data, magnetic measurement and thermal analysis.

Table 2. Element analysis and physicochemical characteristics of ligand and metal complexes.

Compound	The molecular formula Chloride content %	Color	m.p (°C)	Yield %	M.wt g.mol^{-1}	Micro Element Analysis Calc.			Metal content %	Chloride content %
						C%	H%	N%		
L	$C_{23}H_{25}N_5O_5$	White	198-200	95-98	451	60.02 (59.16)	5.8 (5.1)	16.63 (15.69)	_____	_____
C_1 Co(II)	$C_{46}H_{50}N_{10}O_{10}C_OCl_2$	Pale blue	190-192	87-90	1031.93	52.73 (53.49)	5.05 (4.84)	12.75 (13.56)	5.71 (4.4)	6.88 (6.3)
C_2 Ni(II)	$C_{46}H_{50}N_{10}O_{10}NiCl_2$	Light green	186-190	85-92	1031.69	52.68 (52.50)	5.04 (4.84)	15.75 (15.06)	5.68 (4.2)	6.88 (5.78)
C_3 Pt(IV)	$C_{23}H_{25}N_5O_5PtCl_4$	brown	224-228	92-95	788.09	36.01 (35.02)	3.77 (3.1)	9.75 (8.88)	_____	18.01 (17.68)

Table 3. Identifying the ligand and its metal ion complexes by their respective names and chemical formulas.

Comp	Formula	Name
L	$C_{23}H_{25}N_5O_5$	N-(2-((2-amino-4-((3,4,5-trimethoxycyclohexa-1,3-dien-1-yl)methyl)pyrimidin-5-yl)(methyl)amino)-2-oxoethyl)benzamide
C_1 Co(II)	$C_{46}H_{50}N_{10}O_{10}C_OCl_2$	N-(2-((2-amino-4-((3,4,5-trimethoxycyclohexa-1,3-dien-1-yl)methyl)pyrimidin-5-yl)(methyl)amino)-2-oxoethyl)benzamide cobalt chloride
C_2 Ni(II)	$C_{46}H_{50}N_{10}O_{10}NiCl_2$	N-(2-((2-amino-4-((3,4,5-trimethoxycyclohexa-1,3-dien-1-yl)methyl)pyrimidin-5-yl)(methyl)amino)-2-oxoethyl)benzamide Nickle chloride
C_3 Pt(IV)	$C_{23}H_{25}N_5O_5PtCl_4$	N-(2-((2-amino-4-((3,4,5-trimethoxycyclohexa-1,3-dien-1-yl)methyl)pyrimidin-5-yl)(methyl)amino)-2-oxoethyl)benzamide platinum chloride.

FT-IR spectroscopy

Due to ligand interaction with metal ions via the ν (C=O) amide and (C=N) group, the FTIR spectra of ligand complexes (cobalt, nickel, and platinum) revealed a change in the stretching vibration of ν (C=O) amide and (C=N) as shown in Table 4 [17]. Figs. 2–5 display ligand and complex spectra, respectively. Due to the amidation at a lower frequency in the spectra of complexes, which is the result of interaction with metal ions, a new band at 1587 cm^{-1} and the trimethoprim at 1595 cm^{-1} were appeared for the ν (C=N) group of the ligand. New low-frequency stretches were finally attributed to M-N, M-O, and M-Cl (Abdul Ghani & Khaleel 2009; Abdul Ghani & Khaleel 2009).

Table 4. FT- IR spectra of ligand and it complexes.

		υNH2	υN-H amide	υC=O amide	υC=N	υM-CI	υM-N	υM-O
1	Hippuric	_____	3344	1604	____	_____		
2	Trimethoprim	3469asy 3319sy	_____	___	1595	_____		
3	L	3284asy 3186sy	3313	1668	1587	_____		
6	C_1 Co (II)	3342asy 3294sy	3317	1660	1593	349	713	580
5	C_2 Ni (II)	3379asy 3332sy	3313	1662	1593	343	715	582
7	C_3 Pt (IV)	3359asy 3226sy	3315	1633	1595	347	777	579

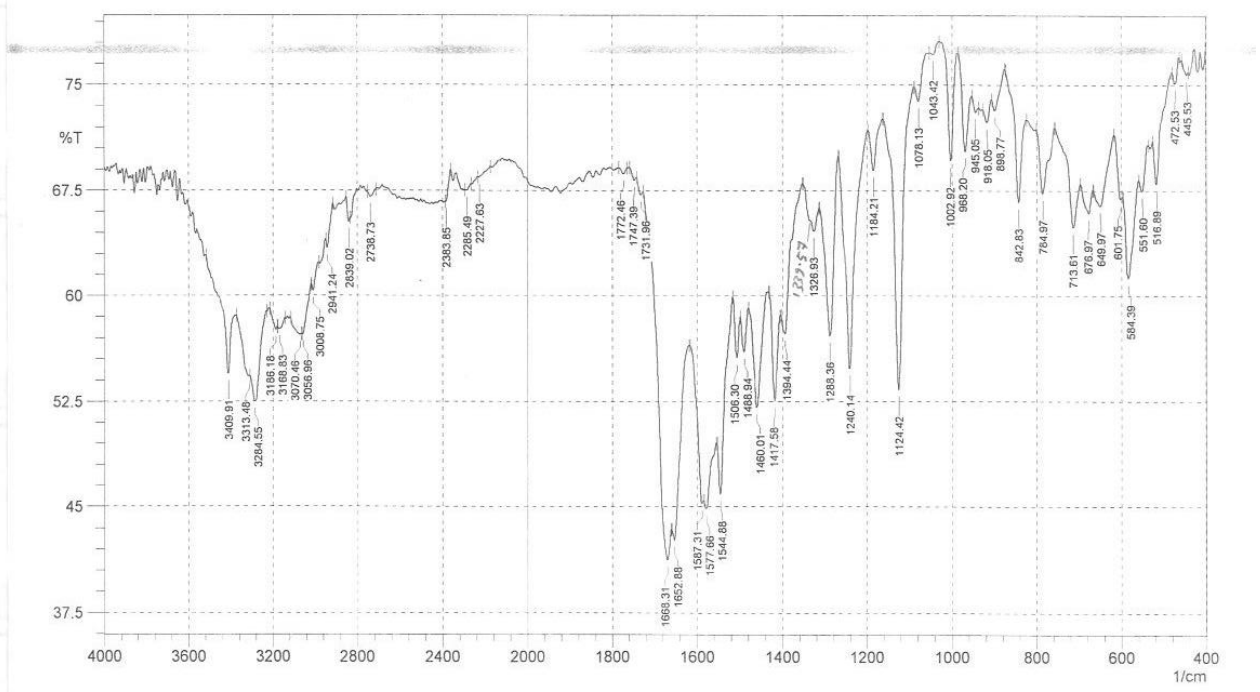

Fig. 2. Spectral analysis of ligands by Fourier transform infrared.

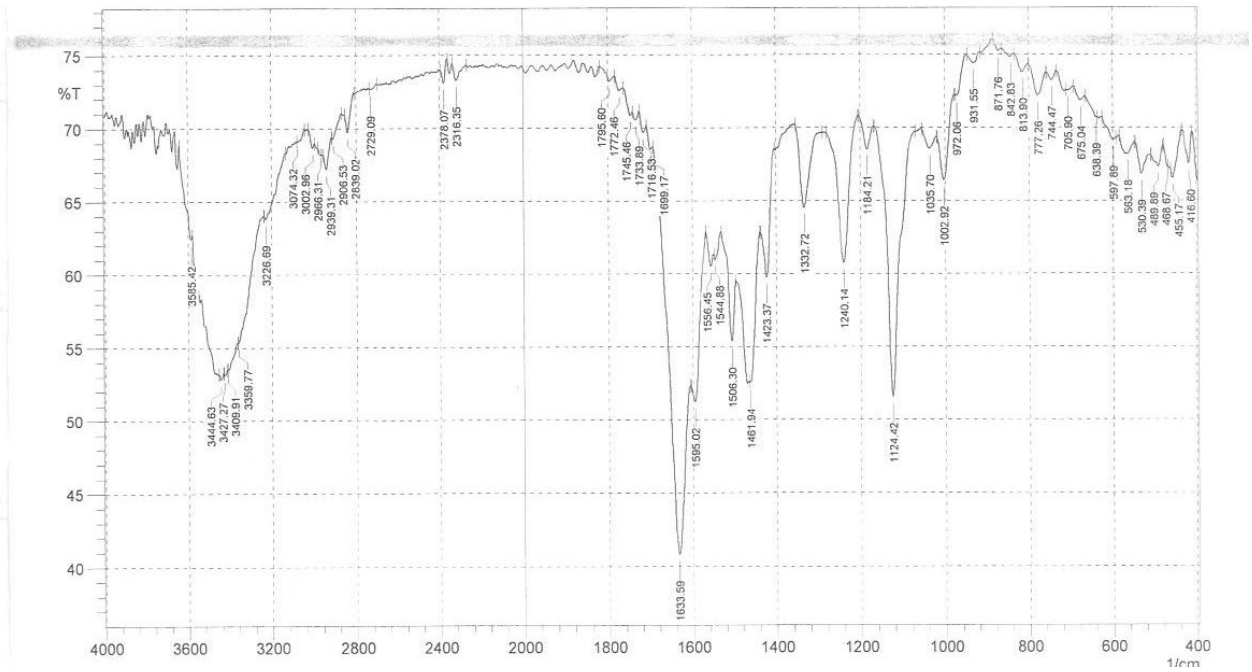

Fig. 3. Fourier transform infrared spectra of a platinum ligand complex.

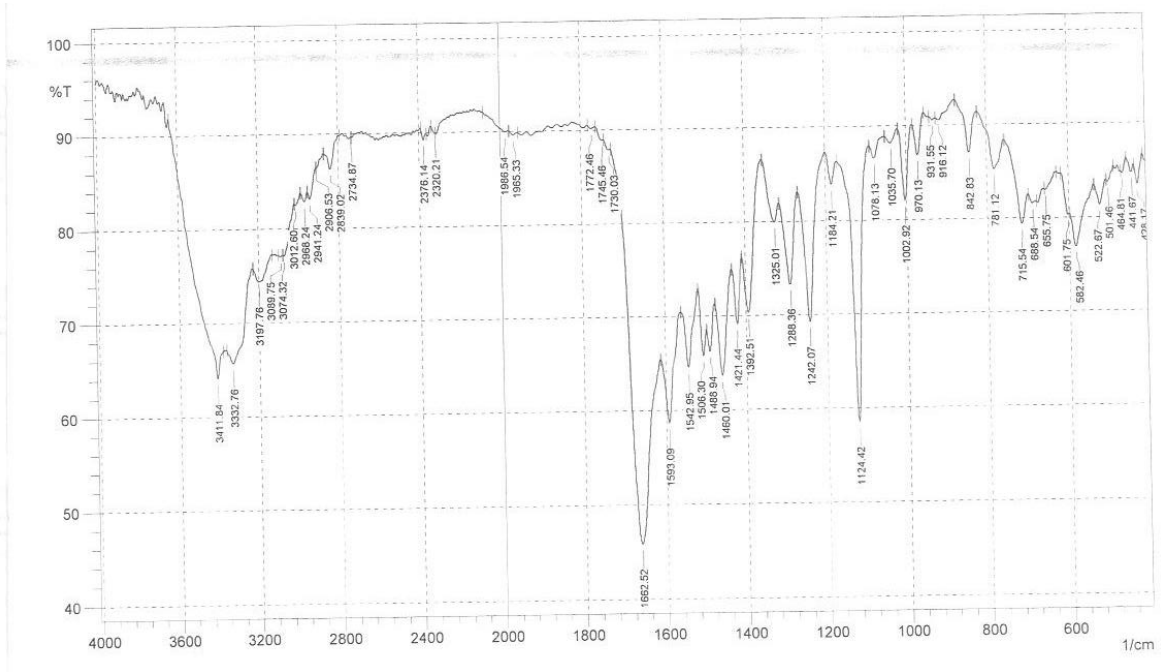

Fig. 4. Spectrum of a Nickel-ligand combination obtained using Fourier transform infrared spectroscopy.

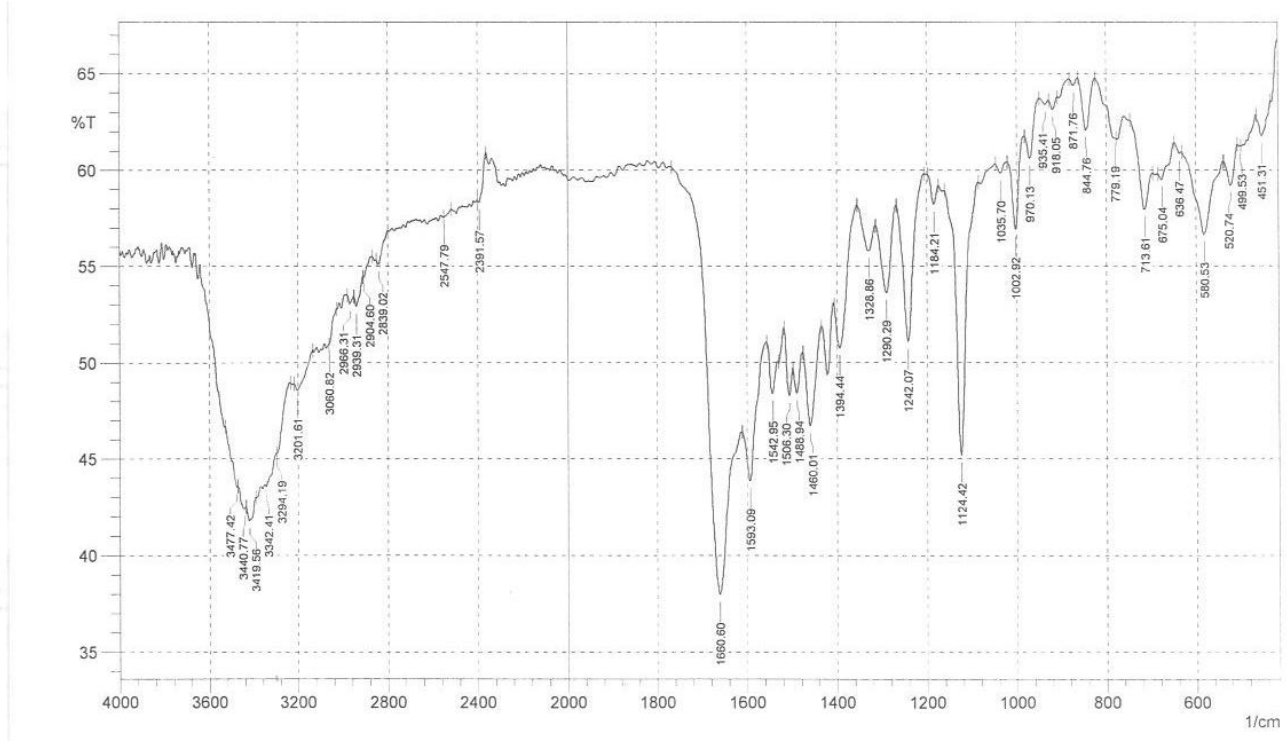

Fig. 5. Fourier transform infrared spectra of a platinum ligand complex.

[1]HNMR spectra

The [1]HNMR spectra of ligand (Figs. 6-7) showed the chemical shift peaks of methylene group, methyl group, aromatic, amine and piperazinyl protons. These peaks were similar to hippuric acid and trimethoprim peaks (Tables 3-4). The amide proton showed a multiple peaks at δ 8.92 ppm, in agreement with literature (Drevenšek *et al.* 2006; Siskos *et al.* 2017)

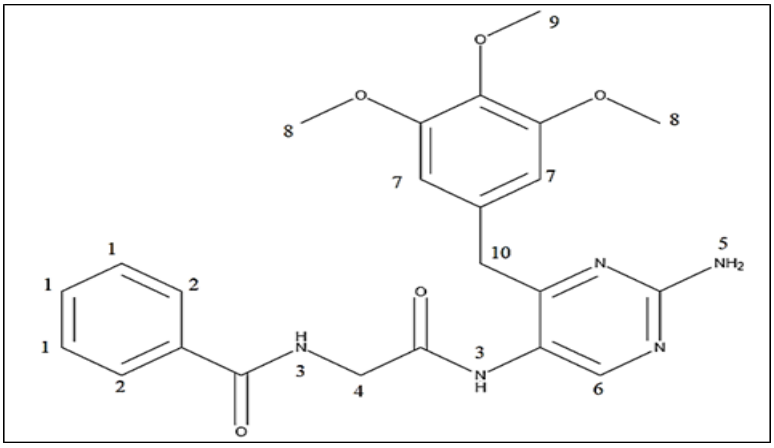

Fig. 6. Structure of the ligand.

Table 3. ^{1}H-NMR data of ligand.

Assignments in d^6 -DMSO	Mark	Chemical shifts δ (ppm)
Methylene protons	10	(3.58), 2H, s
Methyl protons	9	(3.64), 3H, s
Methyl protons	8	(3.87), 6H, s
Aromatic protons	7	(6.62), 2H, s
Amine protons	5	(7.08), 2H, s
Piperazinyl protons	6	(7.48), H, s
Aromatic protons	1,2	(7.72 3H, m -7.89 2H, d)
Amide protons	3	(8.92), 2H, m

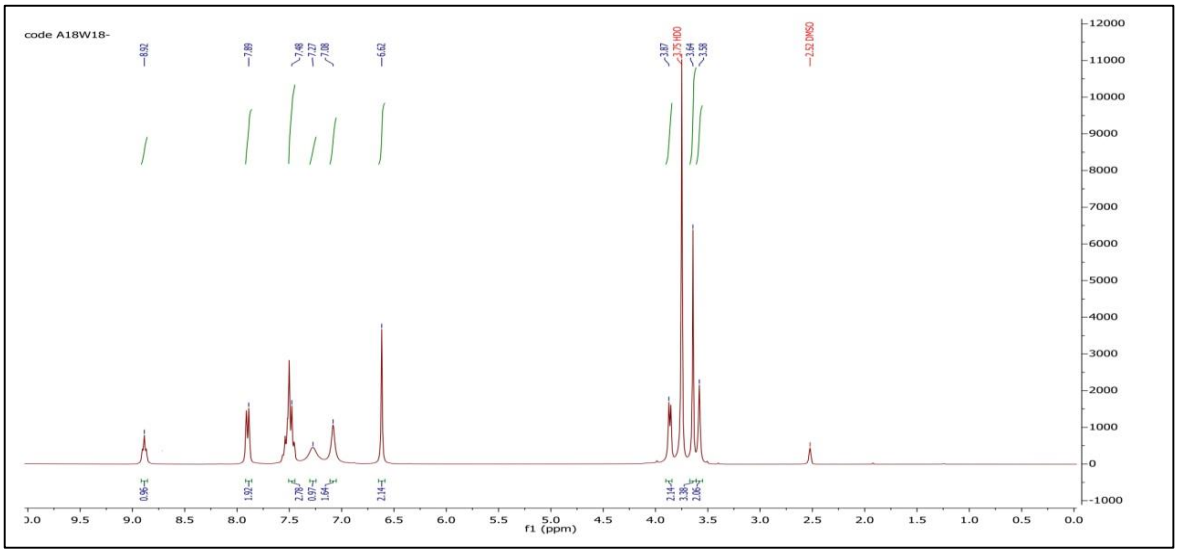

Fig. 7. ^{1}HNMR spectrum of ligand.

Thermal analysis of the ligand and its metal complexes

Argon gas thermogravimetric (TG) and differential thermal analysis (10 °C/min) were performed throughout a temperature range of 25 °C - 800 °C. Table 4 contains thermal dissociation data, while Figs. 8-11 display thermographs of ligand and its metal complexes.

Table 4. Thermal decomposition of the ligand and its complexes.

Comp	Molecular formula and Molecular weight (g mole^{-1})	Steps	Temp. rang of the Decomposition (°C)	Suggested Formula of loss	Mass loss (%) Cal. (Foun)	DTA (°C)
Ligand	$C_{23}H_{25}N_5O_5$ (451)	1	0 -33	$2(OCH_3)+NH_2$	18.41 (17.29)	____
		2	33-300	$C_6H_2+2(CH_2)+OCH_3+C_6H_5+2CO+2NH$	64.84(65.63)	215 (Exo)
		3	300-614	C_3N_2	14.10(14.19)	585 (Exo)
		residue	614-800	CH	2.66(2.88)	____
C_1 (Co)	$C_{46}H_{50}N_{10}O_{10}CoCl_2$ (1031.93)	1	0 - 28	$2Cl+5OCH_3+NH_2$	22.98(23.45)	____
		2	28-302	$OCH_3+2(C_6H_2)+2CH_2+2C_4N_2H+NH_2+2(C_6H_5)+2CO+2NH+CH_2C$	62.80(62.31)	290 (Exo)
		3	302-585	$CoO+NH+CO$	12.78(11.42)	____
		residue	585-800	$NH+CH_2$	1.45(2.81)	590 (Exo)
C_2 (Ni)	$C_{46}H_{50}N_{10}O_{10}NiCl_2$ (1031.69)	1	0 – 38	$2Cl+5(OCH_3)+NH_2$	22.96(23.45)	____
		2	38 – 300	$OCH_3+2(C_6H_2)+2(CH_2)+2(C_4N_2H)+NH_2+2(C_6H_5)+2CO+2NH+CH_2C$	62.55(62.32)	75 (Exo)
		3	300– 567	$NIO+NH+CO$	12.20(11.4)	350 (Exo)
		residue	567-800	$NH+CH_2$	2.29(2.81)	575 (Exo)
C3 (Pt)	$C_{23}H_{25}N_5O_5PtCl_4$ (788.09)	1	0 – 33	2CL	9.076(9.009)	____
		2	33-300	$2Cl+OCH_3$	11.80(12.94)	90 (Exo)
		3	300-357	$2OCH_3+NH_2+C_6H_2+CH_2+C_6H_5$	29.90(30.83)	____
		4	357-493	$2CO+NH+CH_2+NCN$	16.58(15.86)	365 (Exo)
		residue	493-800	$Pt+NH+C_3H$	32.64(31.35)	500 (Exo)

Electronic Spectra

All of the produced compounds' electronic spectra were acquired in methanol (10^{-3} M) at room temperature.

Electronic spectra of ligand

At 244 nm (40983 cm^{-1}) and 272 nm, the ligand's electronic spectra displayed two prominent bands (36764 cm^{-1}; Table 5) due to the π -π* transition. Fig. 12 depicts a spectrum of the ligands.

Electronic spectrum of Co(II) complex (C_1)

Spectrum of the C1 complex showing position change due to interaction with a metal ion (Fig. 13) due to the π-π* transition. Spectra of the C_1 complex revealed bands around 638 nm (15674 cm^{-1}), which were shown to be attributable to the $^4T_1g \rightarrow {}^4A_2g$ and 961 nm (10405 cm^{-1}) describe the $^4T_1g \rightarrow {}^4T_2g$ transitions of the octahedral Co(II) complex.

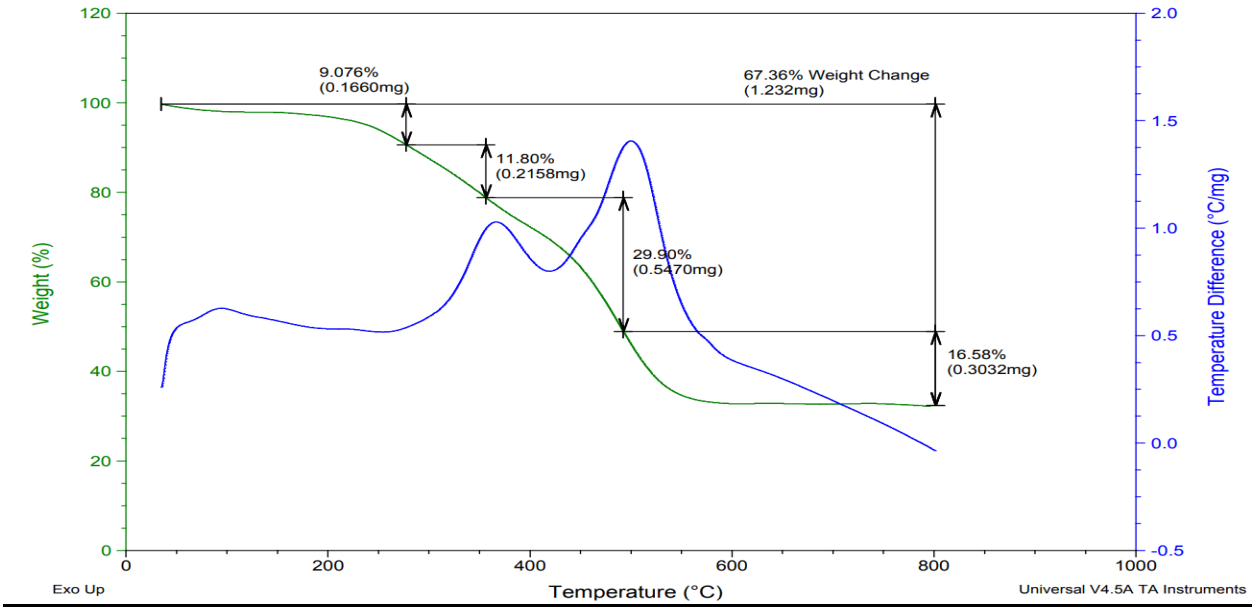

Fig. 8. Thermogram of the ligand.

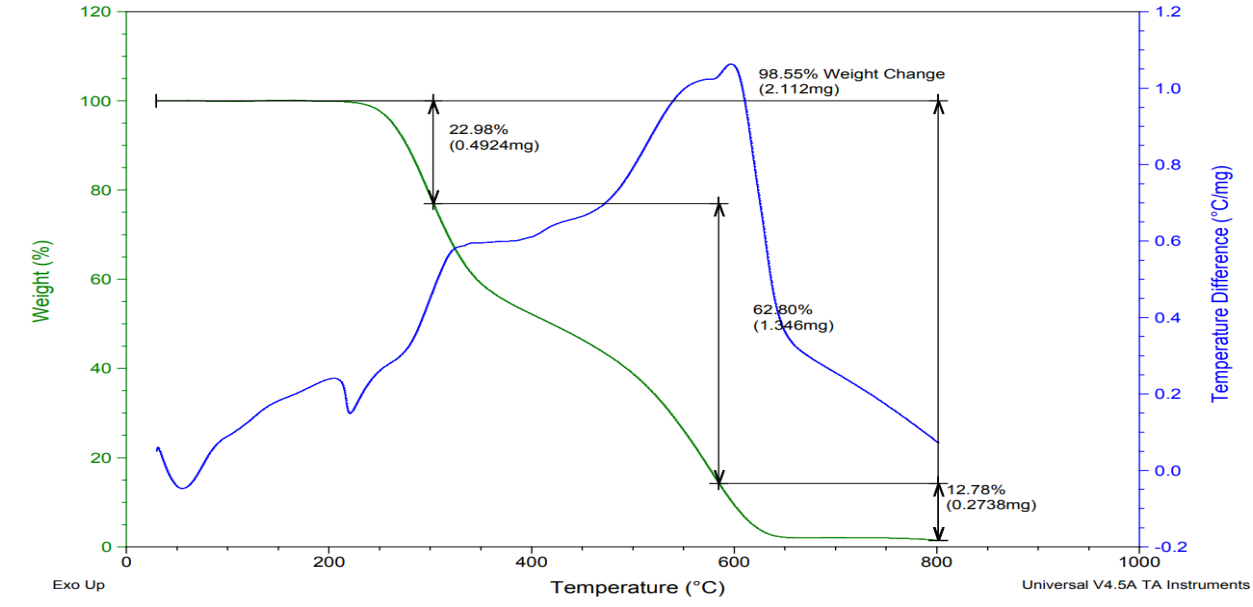

Fig. 9. Thermogram of the cobalt complex of ligand.

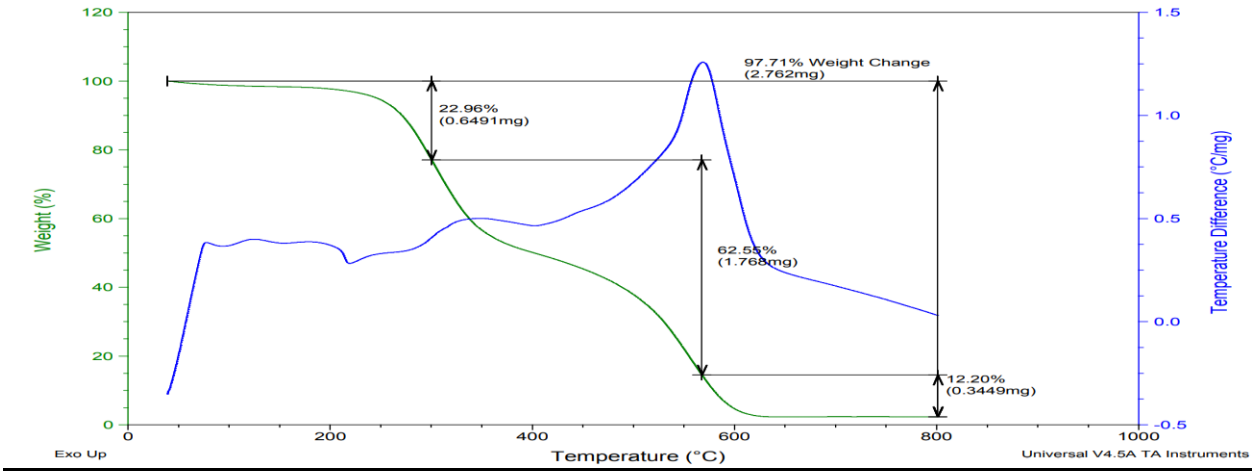

Fig. 10. Thermogram of the nickel complex of ligand.

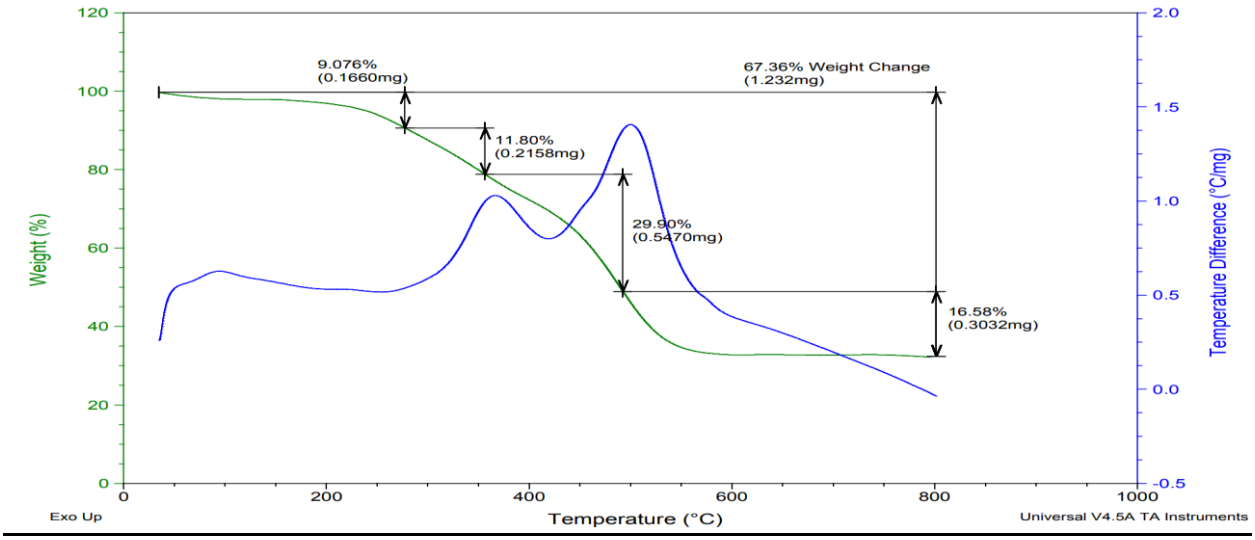

Fig. 11. Thermogram of the platinum complex of ligand.

Electronic spectrum of Ni (II) complex (C_2)

An alteration in the position of the C2 complex was seen in its spectral line (Figure 14) because of π-π* transition due to coordination with metal ions. Bands at 662 (15105 cm^{-1}) and 980 (10204 cm^{-1}) were demonstrated to be present in the C2 complex's spectra to $^3A_2g \rightarrow {}^3T_1g$ and $^3A_2g \rightarrow {}^3T_2g$ transition respectively of octahedral Ni (II) complex (Abdul Ghani & Khaleel 2009).

Electronic spectrum of pt (II) complex (C_3)

A shift in position was seen in the C_3 complex spectra (Fig. 15) of π-π* transition due to coordination with metal ions. Bands in the C_3 complex spectrum were displayed, with peak intensity at 770 nm (12987 cm^{-1}). This band assigned to $^1A_1\ g \rightarrow {}^3T_1g$ transition respectively of octahedral pt (II) complex (Abdul Ghani & Khaleel 2009; Khaleel & Jaafar 2017). All three complexes (C_1, C_2, and C_3) tested negatively for electrolyte conductivity when dissolved in water. The molar conductivity values of H_2O were calculated. 93, 74, and 82 (S cm^2 mol^{-1}), all non-electrolyte values, suggest a C_1, C_2, and C_3 complex (Ali *et al.* 2013).

Table 5. Electronic Spectra of ligand and complexes.

Comp	Band positions nm (cm^{-1})	Assignment	Molar conductivity (S cm^2 mol^{-1}) in H_2O	μeff. (B.M)	Suggested geometry
ligand	244 (40983)	}π →π*		____	___
	272 (36764)				
C_1	269 (37174)	π →π*	93	4.95	
(Co)	247 (40485)				Octahedral
	638 (15674)	$^4T_1g \rightarrow {}^4A_2g$			
	961 (10405)	$^4T_1g \rightarrow {}^4T_2g$			
C_2	230 (43478)	π →π*	74	___	
(Pt)	300 (33333)				
	770 (12987)	$^1A_1\ g \rightarrow {}^3T_1g$			Octahedral
	1036 (96525)				
C_3	247 (40485)	π →π*	82	3.13	Octahedral
(Ni)	272 (36764)				
	980 (10204)	$^3A_2g \rightarrow {}^3T_2g$			
	662 (15105)	$^3A_2\ g \rightarrow {}^3T_1g$			

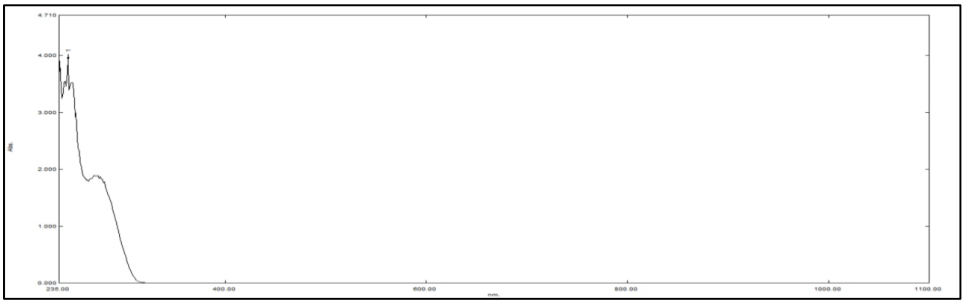

Fig. 12. UV-Vis spectrum of the ligand.

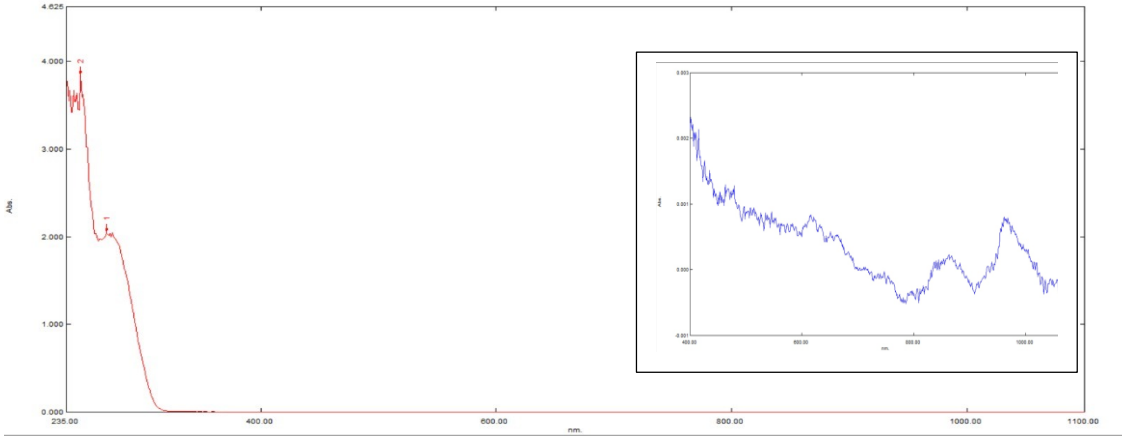

Fig. 13. UV-Vis spectrum of the complex C_1.

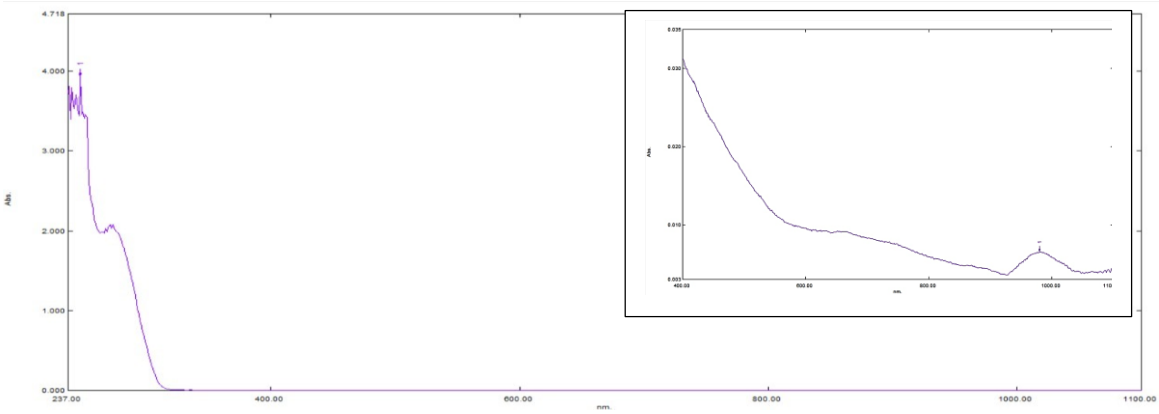

Fig. 14. UV-Vis spectrum of the complex C_2.

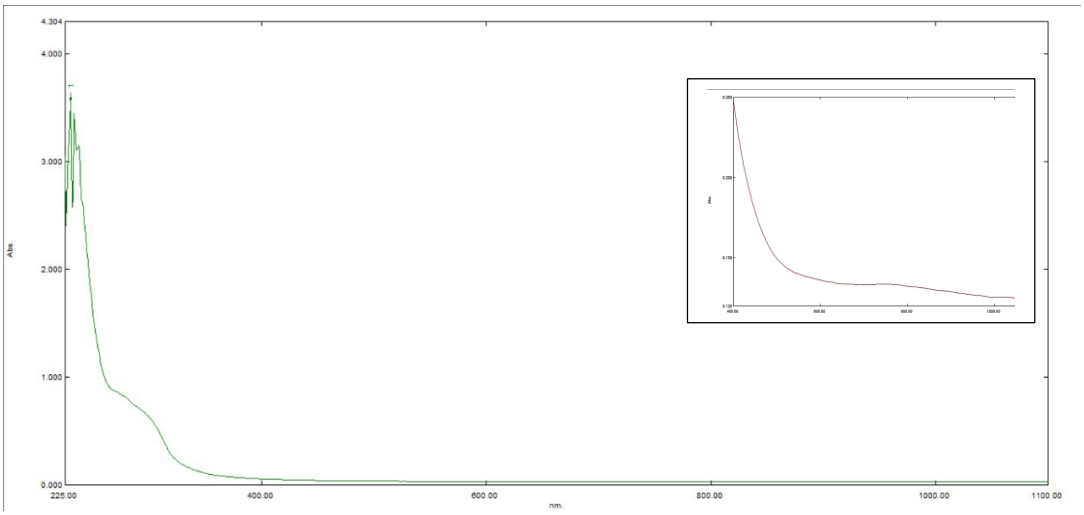

Fig. 15. UV-Vis spectrum of the complex C_3.

Biological activity (Antimicrobial activity)

Using the 10^{-2} M fusion method in DMSO, the ligands and their metal complexes were investigated for their antibacterial properties. Antibacterial and antifungal activity of the produced compounds was tested against *Pseudomonas aeruginosa*, *Staph* and *Candida albicams*. The order of activities for ligand and its complexes was as follow: Pt > ligand CO > ligand Ni >Tri > H> ligand in *Pseudomonas aeruginosa* depending on inhibition zone (30>28>20>18>14>13 mm) respectively, while in *Staphylococcus aureus* the order was exactly the reverse as follow: ligand Ni > ligand >Tri>H> ligand Pt at inhibition zone (27>26>22>17>15>11 mm), respectively. In the case of *Candida albicams* the order was as follow: ligand Ni> ligand CO> ligand Pt> ligand >H> Tri at inhibition zone (29>25>23>21>14>13 mm), respectively.

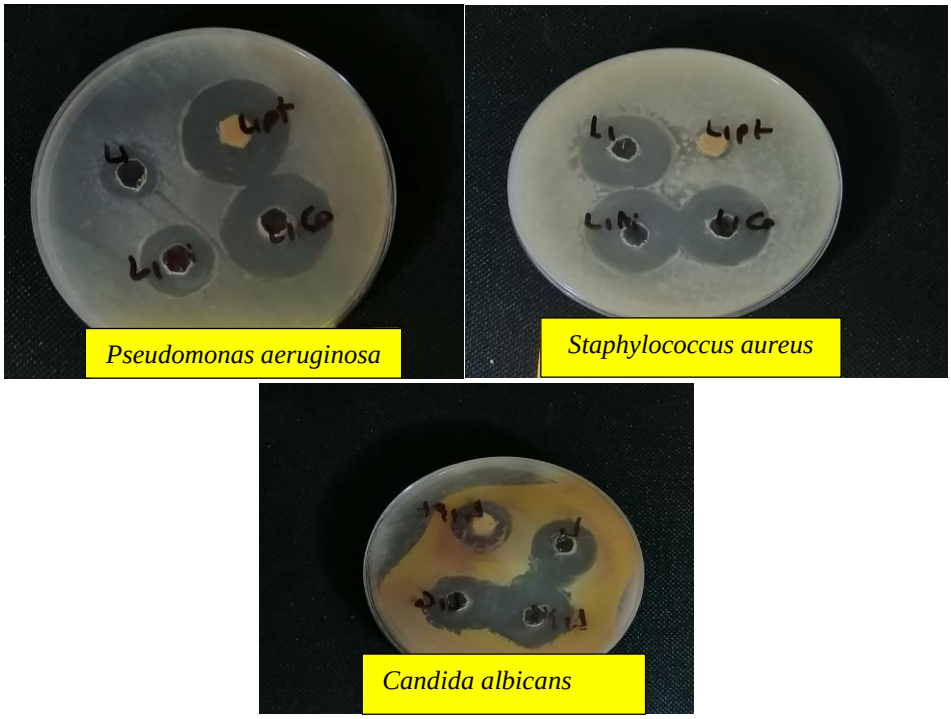

Fig. 7. The inhibition zone for ligand and its complex.

Table 7. The biological activity for studied compounds in (10^{-2}M).

	Pseudomonas aeruginosa	***Staphylococcus aureus***	***Candida albicams***
DMSO	-ve	-ve	-ve
H	14	15	14
Tri	18	17	13
ligand	13	22	21
ligand Ni	20	27	29
ligand CO	28	26	25
ligand Pt	30	11	23

Anticancer

Adenocarcinomic human cells (A549) were used in a 3-(4,5-dimethylthiazol-2-yl)-2,5-diphenyltetrazolium bromide (MTT) assay to test the cytotoxic effect of ligand and complexes. According to the findings, the vitality of A549 cells was inhibited by trimethoprim, ligand, and platinum complex throughout a concentration range of (400-50) g mL^{-1}, while normal cells were very slightly affected at the same doses. The cytotoxic study was performed at 72 h for the ligand, trimethoprim and platinum complex of ligand.

It appears from the preceding data that trimethoprim has a more potent killing effect than ligand and its platinum complex.

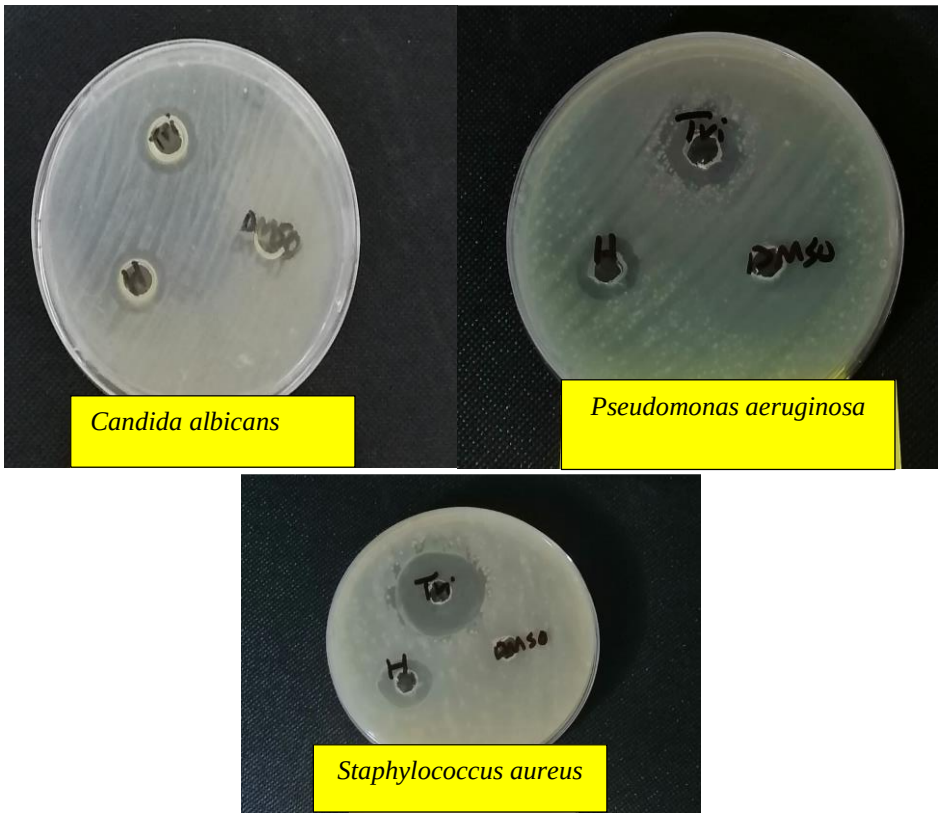

Fig. 8. The inhibition zone for hippuric acid and trimethoprim.

Table 9. Trimethoprim cytotoxic effects on the A549 tumour cell line and a normal cell line HDFn.

Cell line	Conc. (µg mL^{-1})				IC_{50} (µg mL^{-1})	p- value
	400	200	100	50		
A549	32.91	41.09	52.51	62.69	28.91	
	±2.17	±1.34	± 3.69	± 2.89		<0.0001
HDFn	61.42	72.84	83.99	91.59	208.9	
	±1.69	±2	±1.58	± 2.68		

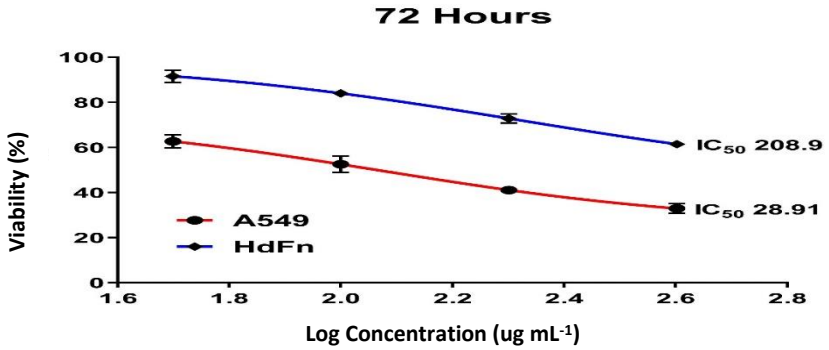

Fig. 10. Effect of trimethoprim on cytotoxicity in A549 cells after 72 h of incubation at 37 ℃ (Log for the original concentration).

Table 10. Analysis of ligand cytotoxicity in A549 tumour cells and a control cell line HDFn.

Cell line	Conc. (µg mL^{-1})				IC_{50} (µg mL^{-1})	p- value
	400	200	100	50		
A549	50.51	60.81	73.96	88.27	71.03	
	±6.23	±4.13	±2.51	±1.62		<0.0001
HDFn	67.75	74.5	87.11	95.95	127.9	
	±2.22	±1.92	±3.02	±1.03		

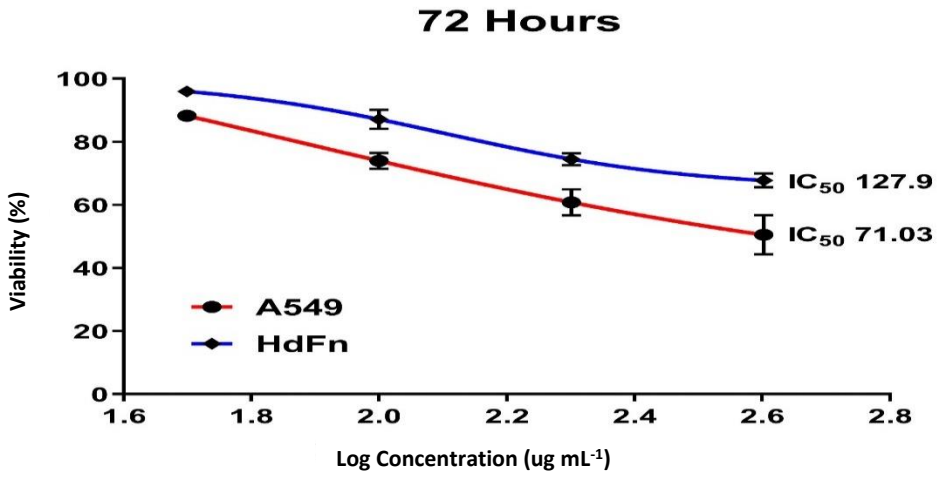

Fig. 10. After 72 h of incubation at 37 ℃, the ligand exhibited a cytotoxic effect on A549 cells (Log for the original concentration).

Table 11. Effects of the ligand pt complex on cytotoxicity in A549 tumour cells and a control cell line HDFn

Cell line	Conc. (µg mL^{-1})				IC_{50} (µg mL^{-1})	p-value
	400	200	100	50		
A549	48.63 ± 8.25	51 ± 3.77	63.81 ± 3.26	75.12 ± 1.95	104.3	<0.0001
HDFn	63.16 ± 2.46	67.07 ± 8.86	80.63 ± 6.22	86.81 ± 2.01	130	

CONCLUSION

A novel amide base ligand is produced from the reaction of trimethoprim with hippuric acid at a molecular ratio of 1:1. All of the compounds synthesized were analysed, and their spectral and physical-chemical properties were used to confirm the suggested structure. The results demonstrated that the ligand complexes of cobalt (II), nickel (II), and platinum (IV) all have an octahedral shape. The pt complex displayed outstanding antibacterial action against *Staphylococcus aureus*, *Pseudomonas aeruginosa*, and *Candida*, as shown by the biological and anticancer outcomes for platinum (IV) complexes. The pt combination that was developed was effective against cancer.

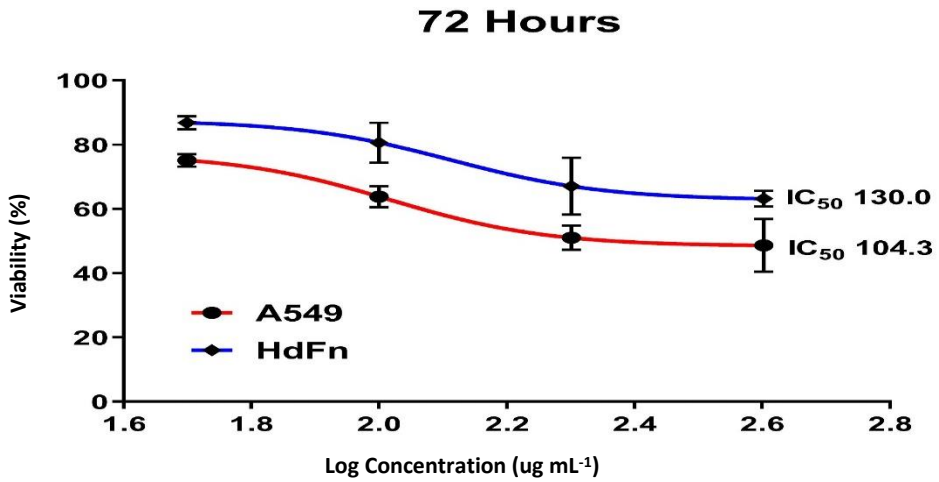

Fig. 12. L1 pt complex cytotoxicity on A549 cells after 72 h of incubation at 37 ℃. (Log for the original concentration).

REFERENCES

Abdul Ghani, AJ & Khaleel, A 2009, Synthesis and characterization of new Schiff bases derived from N (1)-substituted Isatin with dithiooxamide and their co (II), Ni (II), Cu (II), Pd (II), and Pt (IV) Complexes. *Bioinorganic Chemistry and Applications*, 2009: 12.

Abdul Ghani, AJ & Khaleel, AM 2009, Synthesis and characterization of amide and Schiff base derived from N-substituted Isatins and their complexes with some metal ions., pp. 1458-1471.

Ali, I, Wani, WA & Saleem, K 2013, Empirical formulae to molecular structures of metal complexes by molar conductance. *Synthesis and Reactivity in Inorganic, Metal-Organic, and Nano-Metal Chemistry*, 43: 1162-1170. DOI:10.1080/15533174.2012.756898

Aljeboree, AM, Alhattab, ZD, Altimari, US, Aldulaim, AKO, Mahdi, AK & Alkaim, AF 2023, Enhanced removal of amoxicillin and chlorophenol as a model of wastewater pollutants using hydrogel nanocomposite: Optimization, thermodynamic, and isotherm studies. *Caspian Journal of Environmental Sciences*, 21: 411-422

Amdare, MD, Jogdand, KR, Kathane, LL, Kuhite, NG, Padole, CD & Mahapatra, DK 2017, Synthesis of a potential anti-inflammatory pyrazole derivative from hippuric acid as the starting material. *Journal of Pharmaceutical, Chemical and Biological Sciences*, 5: 216-220.

Capasso C & Supuran, CT 2014, Sulfa and trimethoprim-like drugs—antimetabolites acting as carbonic anhydrase, dihydropteroate synthase and dihydrofolate reductase inhibitors. *Journal of Enzyme Inhibition and Medicinal Chemistry*, 29: 379-387.

Chiu, CH, Chen, CT, Cheng, MH, Pao, LH, Wang, C & Wan, GH 2021, Use of urinary hippuric acid and o-/p-/m-methyl hippuric acid to evaluate surgical smoke exposure in operating room healthcare personnel. *Ecotoxicology and Environmental Safety*, 217: 112231.

Cooper, JR, Floyd, EB & Robert, HR 2007, The complete story of the benzodiazepines. Oxford University Press.

Drevenšek, P, Košmrlj, J, Giester, G, Skauge, T, Sletten, E, Sepčić, K, et al. 2006, X-Ray crystallographic, NMR and antimicrobial activity studies of magnesium complexes of fluoroquinolones–racemic ofloxacin and its S-form, levofloxacin. *Journal of Inorganic Biochemistry*, 100: 1755-1763.

Eicher, T & Hauptmann, S 2003, The chemistry of heterocycles: structure, reactions, synthesis, and applications. Wiley-VCH 2nd ed., pp. 159-165.

Goldstein, E 1987, Norfloxacin, a fluoroquinolone antibacterial agent, classification, mechanism of action and in vitro activity. *American Journal of Medicine*, 82(6B): 3-17, DOI: 10.1016/0002-9343(87)90612-7

Guyton & Hall 1975, Text book of medical physiology. Elsevier-Saunders (7th Ed. 2005). 63.

Khaleel, AMN & Jaafar, MI 2017, Synthesis and characterization of boron and 2-aminophenol Schiff base ligands with their Cu (II) and Pt (IV) complexes and evaluation as antimicrobial agents. *Oriental Journal of Chemistry*, 33: 2394-2404.

Mayo CP 2002, Pharmacology of Antidepressants. Vol. 76, 60 p.

Merrill, AH & Henderson, JM 1999, Vitamin B6 metabolism by human liver. *Annals of the New York Academy of Sciences Journal*, 585: 110-117

Mutschler, E 1995, Drug action: Basic principles and therapeutic aspects. Med Pharma Scientific Pub.

Qassem, AA & Jassim, IK 2021, Synthesis of some new maleamic acid and maleimide derivatives of trimethoprim (TMP), with evaluating their biological activity. *Annals of the Romanian Society for Cell Biology*, 25: 1978-1985.

Siskos, MG, Choudhary, MI & Gerothanassis IP 2017, Hydrogen atomic positions of O–H⋯ O hydrogen bonds in solution and in the solid state: The synergy of quantum chemical calculations with 1H-NMR chemical shifts and X-ray diffraction methods. *Molecules*, 22: 415.

Skerritt, JH & Johnston, GA 1993, "Enhancement of GABA binding by benzodiazepines and related anxiolytic." *European Journal of Pharmacology*, 89: 193-98.

UK Food Standards Agency 2008, Vitamin C-Risk Assessment. Retrieved on 2007- 20-19, 55, GF, Combs, The-Vitamins: Fundamental Aspect in Nutrition and Health. San Diego, Elsevier.

Bibliographic information of this paper for citing:

Majeed, AA, Noori Khaleel, AM 2024, Evaluation the anticancer and biological activity by new amide compound of trimethoprim with some of its complexes. Caspian Journal of Environmental Sciences, 22: 9-22.